Genetic Restoration of the Florida Panther
Warren E. Johnson, *et al.*
Science **329**, 1641 (2010);
DOI: 10.1126/science.1192891

Science (print ISSN 0036-8075; online ISSN 1095-9203) is published weekly, except the last week in December, by the American Association for the Advancement of Science, 1200 New York Avenue NW, Washington, DC 20005.

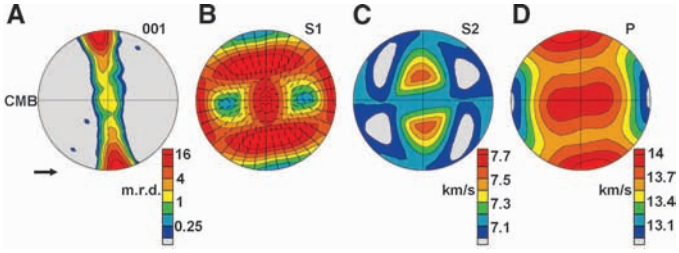

Fig. 3. Equal area projection pole figures showing texture development and anisotropic elastic properties of a pPv aggregate in a subducting slab near the core-mantle boundary using deformation mechanisms established in this study. **(A)** (001) pole figure of pPv showing a snapshot during spreading in a plane strain regime (i.e., intermediate between pure shear and simple shear). **(B)** Fast shear-wave velocities and polarization. **(C)** Slow shear-wave velocities. **(D)** *P* wave velocity surface. Flow direction indicated by arrow.

deformation. Deformation of pPv has been extensively modeled using the viscoplastic self-consistent polycrystal plasticity code [VPSC; (*31*)] (*16*, *17*, *23*). A comparison of the IPFs obtained in this study with results of VPSC models shows that the 001 texture observed here is compatible with dominant slip on (001) lattice planes and 40% compressive strain (Fig. 2D). For this model, the transformation texture obtained after conversion to pPv was used as the starting texture for the deformation simulation (Fig. 2A).

Admittedly, there are limitations to our experiments because the time scale of deformation, grain size, composition, temperature, and deviatoric stress are quite different from those expected in the *D″*. However, if we assume that slip is active on (001) planes in $MgSiO_3$ pPv at *D″* conditions and combine this information with geodynamic modeling of deformation along the *D″*, we can predict texture development in the lowermost mantle. This can, in turn, be combined with single crystal elastic constants to assess associated seismic anisotropy. For these calculations, we neglect any contribution from the second most abundant mineral in the mantle, ferropericlase, which may also play an important role in generating *D″* anisotropy (*32*).

In this context, we use information from the same two-dimensional geodynamic model applied previously (*17*, *33*) to predict texture development in a slab subducted into the *D″* zone. A tracer records the strain-temperature history and, accordingly, the texture evolution is modeled with the same polycrystal plasticity theory applied to the experiment (*31*). It is assumed that the aggregate has a random orientation distribution as it enters the *D″* about 290 km above the CMB. Based on our results, we assume dominant (001)[100] and (001)[010] slip. We chose a geodynamic tracer that records strain and temperature, which advances close to the CMB and attains large strains. Preferred orientation develops rapidly and then stabilizes; note the strong alignment of (001) lattice planes slightly inclined to the CMB (Fig. 3A). By averaging the orientation distribution and single crystal elastic properties (*34*), we calculated aggregate elastic properties and seismic wave propagation. Based on the polarization directions of the fast and slow shear-wave velocities, high shear-wave splitting is 0.55 km/s in the flow direction; fast shear waves are polarized parallel to the CMB (Fig. 3B, C). This is consistent with seismic observations of the circum-Pacific regions (*2*, *4*), where the presence of pPv is expected (*35*, *36*). The anticorrelation between fast *S* waves and *P* waves in the flow direction (Fig. 3D) is also consistent with seismic records (*37*, *38*).

References and Notes

1. D. Helmberger, T. Lay, S. Ni, M. Gurnis, *Proc. Natl. Acad. Sci. U.S.A.* **102**, 17257 (2005).
2. J. Wookey, J. Kendall, in *Post-Perovskite: The Last Mantle Phase Transition*, K. Hirose, D. Yuen, T. Lay, J. P. Brodholt, Eds. (American Geophysical Union, Washington DC, 2007), pp. 171–189.
3. E. J. Garnero, A. K. McNamara, *Science* **320**, 626 (2008).
4. M. Panning, B. Romanowicz, *Science* **303**, 351 (2004).
5. P. J. Tackley, *Science* **288**, 2002 (2000).
6. A. K. McNamara, P. E. V. Keken, S. Karato, *J. Geophys. Res.* **108**, (B5), 2230 (2003).
7. N. Loubet, N. M. Ribe, Y. Gamblin, *Geochem. Geophys. Geosyst.* **10**, Q10004 (2009).
8. M. Murakami, K. Hirose, K. Kawamura, N. Sata, Y. Ohishi, *Science* **304**, 855 (2004).
9. A. R. Oganov, S. Ono, *Nature* **430**, 445 (2004).
10. S. Shim, T. S. Duffy, R. Jeanloz, G. Shen, *Geophys. Res. Lett.* **31**, L10603 (2004).
11. M. Murakami, K. Hirose, N. Sata, Y. Ohishi, *Geophys. Res. Lett.* **32**, L03304 (2005).
12. T. Lay, *Geophys. Res. Lett.* **35**, L03304 (2008).
13. K. Ohta, K. Hirose, N. Sata, Y. Ohishi, *Geochim. Cosmochim. Acta* **70**, A454 (2006).
14. K. Catalli, S. H. Shim, V. Prakapenka, *Nature* **462**, 782 (2009).
15. D. Andrault *et al.*, *Earth Planet. Sci. Lett.* **293**, 90 (2010).
16. S. Merkel *et al.*, *Science* **311**, 644 (2006).
17. S. Merkel *et al.*, *Science* **316**, 1729 (2007).
18. T. Okada, T. Yagi, K. Niwa, T. Kikegawa, *Phys. Earth Planet. Inter.* **180**, 195 (2010).
19. N. P. Walte *et al.*, *Geophys. Res. Lett.* **36**, L04302 (2009).
20. N. Miyajima, K. Ohgushi, M. Ichihara, T. Yagi, *Geophys. Res. Lett.* **33**, L12302 (2006).
21. D. Yamazaki, T. Yoshino, H. Ohfuji, J. Ando, A. Yoneda, *Earth Planet. Sci. Lett.* **252**, 372 (2006).
22. K. Niwa *et al.*, *Phys. Chem. Miner.* **34**, 679 (2007).
23. L. Miyagi *et al.*, *Earth Planet. Sci. Lett.* **268**, 515 (2008).
24. J. Hustoft, S. Shim, A. Kubo, N. Nishiyama, *Am. Mineral.* **93**, 1654 (2008).
25. T. Tsuchiya, J. Tsuchiya, *Phys. Rev. B* **76**, 144119 (2007).
26. P. Carrez, D. Ferré, P. Cordier, *Philos. Mag.* **87**, 3229 (2007).
27. A. Metsue, P. Carrez, D. Mainprice, P. Cordier, *Phys. Earth Planet. Inter.* **174**, 165 (2009).
28. Materials and methods are available as supporting material on *Science* Online.
29. L. Lutterotti, S. Matthies, H. Wenk, A. S. Schultz, J. W. Richardson, *J. Appl. Phys.* **81**, 594 (1997).
30. J. Santillán, S. Shim, G. Shen, V. B. Prakapenka, *Geophys. Res. Lett.* **33**, L15307 (2006).
31. R. Lebensohn, C. Tomé, *Mater. Sci. Eng. A* **175**, 71 (1994).
32. M. D. Long, X. Xiao, Z. Jiang, B. Evans, S. Karato, *Phys. Earth Planet. Inter.* **156**, 75 (2006).
33. A. K. McNamara, S. Zhong, *Nature* **437**, 1136 (2005).
34. S. Stackhouse, J. P. Brodholt, J. Wookey, J. Kendall, G. D. Price, *Earth Planet. Sci. Lett.* **230**, 1 (2005).
35. J. W. Hernlund, C. Thomas, P. J. Tackley, *Nature* **434**, 882 (2005).
36. R. D. van der Hilst *et al.*, *Science* **315**, 1813 (2007).
37. G. Masters, G. Laske, H. Bolton, A. M. Dziewonski, in *Earth's Deep Interior: Mineral Physics and Tomography From the Atomic to Global Scale*, S.-I. Karato, A. M. Forte, R. C. Liebermann, G. Masters, L. Stixrude, Eds. (American Geophysical Union, Washington DC, 2000), pp. 63–87.
38. M. Ishii, J. Tromp, *Phys. Earth Planet. Inter.* **146**, 113 (2004).

39. The Advanced Light Source is supported by the Director, Office of Science, Office of Basic Energy Sciences, and Materials Sciences Division of the U.S. Department of Energy under contract DE-AC02-05CH11231. This research was partially supported by the Consortium for Materials Properties Research in Earth Sciences under NSF Cooperative Agreement EAR 06-49658. L.M. acknowledges support of the Bateman Fellowship at Yale University. H.R.W. acknowledges support from CDAC and NSF grants EAR0836402 and EAR0757608. We thank S. Gaudio, C. Lesher, S. Clark, J. Knight, and J. Yan for technical assistance. Comments from three anonymous reviewers improved the manuscript.

Supporting Online Material

www.sciencemag.org/cgi/content/full/329/5999/1639/DC1
Materials and Methods
Figs. S1 and S2
Tables S1 and S2
References

18 May 2010; accepted 20 August 2010
10.1126/science.1192465

Genetic Restoration of the Florida Panther

Warren E. Johnson,[1]*† David P. Onorato,[2]*† Melody E. Roelke,[3]* E. Darrell Land,[2]* Mark Cunningham,[2] Robert C. Belden,[4] Roy McBride,[5] Deborah Jansen,[6] Mark Lotz,[2] David Shindle,[2] JoGayle Howard,[8] David E. Wildt,[8] Linda M. Penfold,[9] Jeffrey A. Hostetler,[10] Madan K. Oli,[10] Stephen J. O'Brien[1]†

The rediscovery of remnant Florida panthers (*Puma concolor coryi*) in southern Florida swamplands prompted a program to protect and stabilize the population. In 1995, conservation managers translocated eight female pumas (*P. c. stanleyana*) from Texas to increase depleted genetic diversity, improve population numbers, and reverse indications of inbreeding depression. We have assessed the demographic, population-genetic, and biomedical consequences of this restoration experiment and show that panther numbers increased threefold, genetic heterozygosity doubled, survival and fitness measures improved, and inbreeding correlates declined significantly. Although these results are encouraging, continued habitat loss, persistent inbreeding, infectious agents, and possible habitat saturation pose new dilemmas. This intensive management program illustrates the challenges of maintaining populations of large predators worldwide.

Pumas (also called cougars, mountain lions, or panthers) are currently distributed throughout western North America and much of Central and South America (*1*). The endangered Florida panther (listed in 1967, table S1), the last surviving puma subspecies in eastern North Amer-

ica, is restricted to shrinking habitat between the urban centers of Miami and Naples (Fig. 1). By the early 1990s, the population of ~20 to 25 adults (*2*) showed reduced levels of molecular genetic variation relative to other puma populations (*3*–*5*), which is indicative of inbreeding (*4*, *6*). This may have led to defects, including poor sperm quality and low testosterone levels (*4*, *7*), poor fecundity and recruitment (*4*, *7*), cryptorchidism [where >80% of males born from 1990 to 1992 had one or no descended testes (*4*)], a high incidence of thoracic cowlicks and kinked tails (*4*), numerous atrial septal defects (*4*, *8*), and a high load of parasites and infectious disease pathogens (*4*, *8*–*10*).

In 1995, these cumulative observations, coupled with demographic models predicting a 95% likelihood of extinction within two decades, motivated the translocation of 8 wild-caught Texas (TX) female pumas into habitat occupied by at least 22 adult canonical (last-remaining, authentic) Florida panthers (CFPs) and 4 Everglades Florida panthers (EVGs) (Fig. 1A), because historically, gene flow occurred between Texas and Florida puma populations (*11*, *12*).

[1]Laboratory of Genomic Diversity, National Cancer Institute, Frederick, MD 21702, USA. [2]Florida Fish and Wildlife Conservation Commission, Naples, FL 34114, USA. [3]SAIC-Frederick, Laboratory of Genomic Diversity, National Cancer Institute, Frederick, MD 21702, USA. [4]U.S. Fish and Wildlife Service, Vero Beach, FL 32960, USA. [5]Livestock Protection Company, Alpine, TX 79832, USA. [6]Big Cypress National Preserve, Ochopee, FL 34141, USA. [8]Smithsonian Conservation Biology Institute, Front Royal, VA 22630, USA. [9]White Oak Conservation Center, Yulee, FL 32046, USA. [10]Department of Wildlife Ecology and Conservation, University of Florida, Gainesville, FL 32611, USA.

*These authors contributed equally to this work.
†To whom correspondence should be addressed. E-mail: stephenobrien@nih.gov (S.J.O.); warjohns@mail.nih.gov (W.E.J.); Dave.Onorato@MyFWC.com (D.P.O.)

We compared data from 591 individuals sampled from 1978 to 2009 (table S2). Twenty-three informative (minimum allele frequency > 0.1) short tandem repeat (STR) loci were examined to reconstruct genetic heritage and parentage relationships; assess spatial and demographic patterns; distinguish CFP from other puma lineages; track morphological, biomedical, and life history traits as indices of fitness; and associate genetic heritage and heterozygosity with panther survival (*13*).

Pumas of diverse ancestry, time periods, and geographic origins, including wild-caught and captive animals in Florida, clustered into phylogenetic groups (Fig. 2). This analysis, combined with Bayesian population genetic results from STR genotypes that revealed nine distinct groups (fig. S1 and table S2), allowed us to explicitly infer the genetic heritage of each Florida panther (table S2, column 2; Figs. 1 and 2; and fig. S2) and to distinguish the two pre-1995 groups (CFP and EVG). Further, admixed Florida panthers (AdmFPs) were clearly identifiable, including first-generation (F_1) offspring of TX females bred by CFP or EVG males (CFPxTX-F_1 or EVGxTX-F_1) and panthers that were related to captive pumas of western U.S. origin who had escaped from enclosures on the Big Cypress Seminole Indian Reservation (SEM) from 1997 to 1999 (Figs. 1 and 2).

From 1986 to 1995, the minimum number of adult (>1.5 years old) panthers fluctuated from 24 to 32 (Fig. 3A), and genetic heritage remained relatively stable (85% CFP and 15% EVG; Fig. 1 and figs. S1 and S3). After their introduction, five of eight TX females bred (Fig. 1a) and produced 15 F_1 kittens with CFP, EVG, and at least five TX-backcross (TX-BC) offspring (figs. S3 and S4 and table S2). Twelve F_1 panthers produced offspring. From 1995 to 2008, 424 panther births were documented (81 CFP, 319 AdmFP, and 24 undetermined; 272 were observed only as neonatal kittens). These largely AdmFP were responsible for colonizing former panther range and densities increased. For example, between 1995 and 2007, the number and density of panthers in the southern Big Cypress National Preserve (BCNP) (2174 km^2) increased eightfold from 3 (0.14/100 km^2) to 25 (1.15/100 km^2) (Fig. 1).

From 1996 to 2003, numbers (*N*) increased by 14%/year to at least 95 adults (Fig. 3A), 26.6 kittens were produced annually (fig. S2). The effective population size (N_e) rose from 16.4 in 1995 to 32.1 by 2007, and N_e/N was 0.314 (Fig. 1) (*13*). This paralleled an increase in average individual STR heterozygosity (to 25% from 18.4% in 1993; Fig. 3B) and a decrease in the average estimated age of adults from 6.6 to 4.2 years from 1997 to 2004. Population growth slowed and average age increased gradually after 2004 (Fig. 3C).

Admixed genetic ancestry was associated with increased survival of F_1, EVG-BC, and TX-BC kittens (<1 year old) relative to purebred CFP and CFP-backcross (CFP-BC) kittens (0.518 ± 0.130 versus 0.243 ± 0.074, $P = 0.020$) (Fig. 3D). F_1 adults had significantly higher survival ($P = 0.002$) than other admixed or CFP groups (table S4), with a risk ratio (RR: relative instantaneous probability of mortality) of 0.118 (*13*). The survival of subadults and adults increased significantly with heterozygosity (RR for an increase of 0.1 = 0.643, $P = 0.011$). Interestingly, CFPs also experienced significantly higher mortality rates from intraspecific aggression than did AdmFPs (RR = 3.077, $P = 0.014$), and mortality rates from intraspecific aggression declined as heterozygosity increased (RR = 0.480, $P = 0.005$) (*13*).

Demographic differences among >1-year-old panthers from 2002 to 2004 (Fig. 3A) were evident when 23 out of 29 (23/29) (79%) CFPs alive in 2002 were lost versus 22/47 (47%) AdmFPs and when CFPs had a significantly

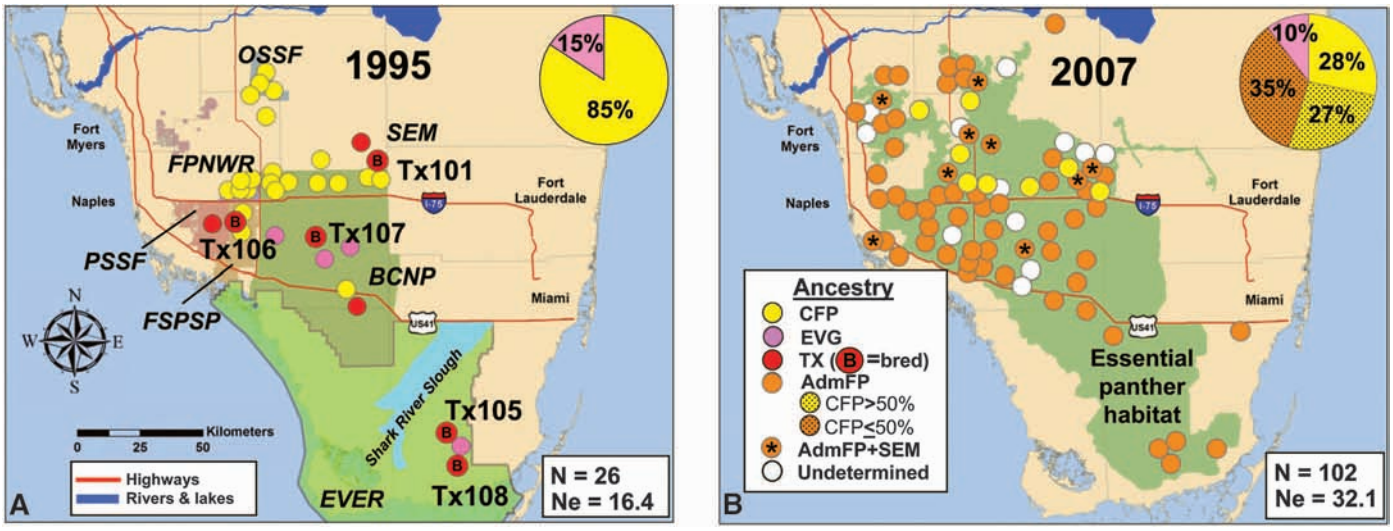

Fig. 1. (**A** and **B**) Southern Florida (1995, left; 2007, right) with locations of breeding-age Florida panthers (>1.5 years old), geographic features, number (*N*) alive, and effective population size (N_e). Labeled colored areas in (A) demarcate public land (*23*): Fakahatchee Strand Preserve State Park (FSPSP), Picayune Strand State Forest (PSSF), Florida Panther National Wildlife Refuge (FPNWR), BCNP, Big Cypress Seminole Indian Reservation (SEM), Okaloacoochee Slough State Forest (OSSF), and Everglades National Park (EVER) and in (B) show panther habitat. Circles are coded by ancestry: CFP, TX females (with a B if a successful breeder), EVG, AdmFP, and SEM. Pie charts illustrate the genetic heritage of the population (fig. S1 and table S2) (*13*).

lower yearly survival (likelihood-ratio test χ^2 = 5.38, P = 0.020), dropping from 0.827 ± 0.044 (from 1997 to 2001) to 0.610 ± 0.087 [AdmFP survival declined from 0.904 ± 0.046 to 0.866 ± 0.027 (P = not significant)]. The number of documented CFP kittens went from 17 in 2002 to 5 total from 2003 to 2005, and none have been observed since (fig. S2). The CFP contribution to the AdmFP population also decreased, with only four litters (14 kittens) of CFPxAdmFP parents documented after 2004. The abrupt CFP decline (versus AdmFP increases; Fig. 3A) and differential patterns of survival and mortality are consistent with an AdmFP competitive advantage.

Panther survival is also affected by disease agents (*4*, *9*). From 2001 to 2007, 19 Florida panthers tested positive for feline leukemia virus (FeLV) antibodies, and 5 in Okaloacoochee Slough State Forest (OSSF) (Fig. 1) died with active FeLV infections (*10*). A capture and vaccination program was implemented in 2003, and no further active infections were documented after July 2004. Further, the prevalence of a puma-specific strain of feline immunodeficiency virus (FIV_{PCO}) increased 16 to 80% from 1995 to 2005. Although not explicitly implicated in clinical disease in free-ranging pumas, FIV_{PCO} infection may predispose individuals to other diseases due to low lymphocyte numbers (*14*).

A detailed population pedigree confirmed all dam/offspring inferences from field observations (278 kittens from 128 litters marked as neonates, and 51 juveniles and subadults associated with suspected dams), supported 120 of 130 sire/offspring field inferences, and identified an additional 174 probable parents (48 dams and 126 sires). At least one parent was assigned to 422 individuals: 74 different dams and 49 sires to 397 and 298 offspring, respectively (table S2 and figs. S3 and S4). The estimated relative genetic contribution of the TX females to the descendant population varied widely (TX101 = 0.20, TX105 = 0.01, TX106 = 0.06, TX107 = 0.10, and TX108 = 0.04).

Shrinking and fragmented populations are at high risk for inbreeding depression (*15*, *16*) and local extinction (*17*) through demographic and stochastic events (*18*). These influences probably caused the precipitous decline in Florida panther N_e from 1900 to 1980 (*19*). The stated goal of the Florida panther genetic restoration plan was to improve population size and viability by increasing genetic variability without losing unique local adaptations. By several measures, this experiment was successful. Most notably, after the introduction of Texas females, the population tripled, with a parallel significant reduction in the incidence of several phenotypic characters historically associated with inbreeding depression (Table 1). Additionally, admixed panthers exhibited behaviors that might be associated with higher fitness, as evidenced by increased escape behavior from high trees during capture (RR = 2.0, P = 0.001, fig. S5).

In addition to genetic restoration, enhancement in panther numbers was probably facilitated by action initiated in the late 1980s by federal, state, and private groups to mitigate panther declines and facilitate natural recovery. This included buttressing legal protection under the Endangered Species Act (*20*), acquiring and protecting >120,000 ha of occupied panther habitat, altering prey management (*21*), and constructing highway underpasses to reduce mortality from vehicle strikes (*22*). In

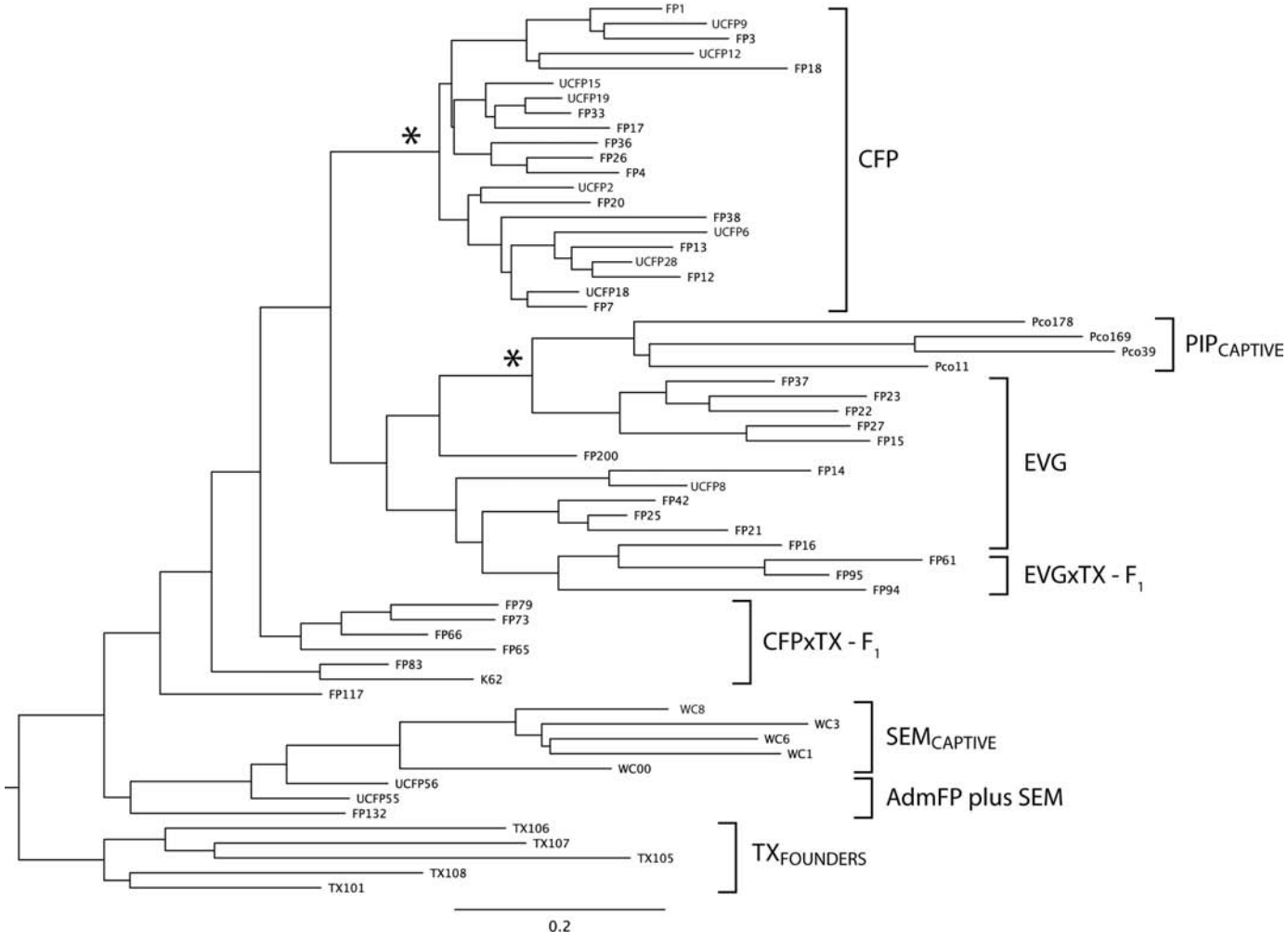

Fig. 2. Neighbor-joining tree of composite STR genotypes portraying genetic relationships among pre-1995 founding CFPs, introduced TX females, EVG and F_1 admixed Florida panthers (CFPxTX-F_1 and EVGxTX-F_1). Captive Piper panthers ($PIP_{captive}$) are related to present-day EVGs through individuals released into the Everglades between 1957 and 1967 (*3*, *4*), and SEMs contributed unintended gene flow. Asterisks mark nodes with >80% bootstrap support (*13*).

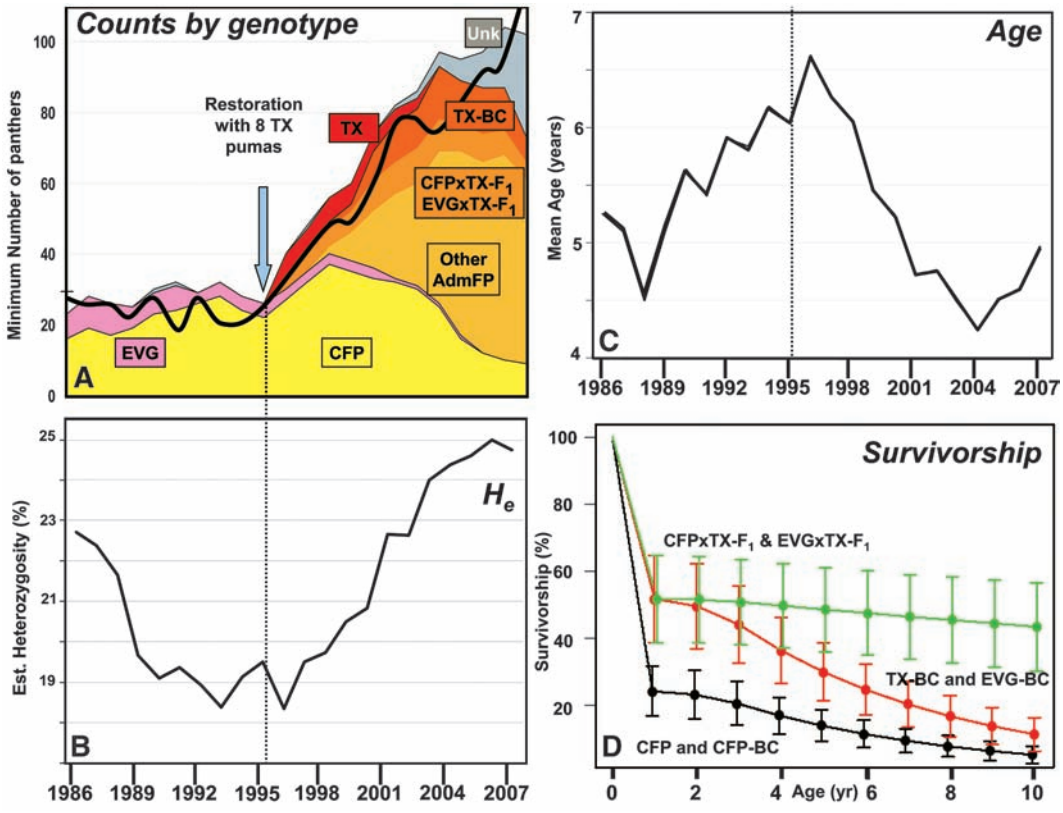

Fig. 3. (**A**) Minimum annual subadult and adult panther population size and inferred genetic heritage from 1986 to 2007. CFPs are yellow, EVGs pink, TXs red, CFPxTX-F_1s and EVGxTX-F_1s orange, TX-BCs and other AdmFPs shades of orange, and genetically uncharacterized individuals (Unk) gray (*13*). The black line is an independent minimum-count estimate from surveys of tracks, spoor, and other field evidence (*2*). (**B**) Mean yearly adult multilocus heterozygosity. (**C**) Yearly mean age of adults. (**D**) Projected survivorship (probability of surviving to an age) curves for female Florida panthers of different genetic heritages with standard error bars (*13*). Male trends are similar (table S4).

Table 1. Estimates of molecular genetic variation and prevalence of physiological and morphologic traits in Florida panthers of different genetic heritages (*13*) (see table S3). NA, not available.

			Crytorchidism**			Prevalence of**			
Heritage group	No.	Average* heterozygosity	Avg. no. of descended testicles	Prevalence in males	Normal sperm (%) Ejaculate (EJ) Gamete rescue (GR) (No. of males)	Atrial septal defects	Kinked tails	Cowlick on thorax	Percent of** individuals with ≥1 abnormal trait
CFP	116	0.167 ± 0.005^{A}	1.3 ± 0.07^{A}	0.66 ± 0.06^{A}	EJ 5.4 ± 0.7^{C} (15) GR 10.1 ± 1.9^{N} (13)	0.17 ± 0.05^{A}	0.90 ± 0.03^{A}	0.81 ± 0.04^{A}	70.3 ± 2.5^{A}
EVG	17	0.282 ± 0.022^{B,D}	2.0 ± 0^{B}	0^{B}	9.5 ± 0.6^{B} (5)	0^{A}	0.31 ± 0.12^{B}	0.29 ± 0.11^{B}	22.5 ± 7.1^{B}
TX	5	0.318 ± 0.02^{B,D}	2.0 ± 0^{B}§	0^{B}§	14.0 ± 3.5^{A,B}§ (9)	0^{A}	0^{B}	0^{B}	0^{B}
All AdmFP	143	0.244 ± 0.006^{B}	1.9 ± 0.0^{B}	0.10 ± 0.035^{B}	(See below)	0.08 ± 0.030^{A}	0.25 ± 0.037^{B}	0.27 ± 0.039^{B}	19.5 ± 2.1^{B}
AdmFP groups									
TX-F_1	10	0.336 ± 0.01^{B,}	2.0 ± 0	0^{B}	EJ 20.5 ± 4.5^{A} (2)	0^{A}	0^{B}	0.38 ± 0.18^{B}	14.6 ± 7.3^{B}
TX-BC	18	0.273 ± 0.016^{B,D}	2.0 ± 0^{B}	0^{B}	NA	0.14 ± 0.14^{A}	0^{B}	0.06 ± 0.06^{B}	3.2 ± 2.2^{B}
Other AdmFP	52	0.251 ± 0.008^{C,D}	1.94 ± 0.04^{B}	0.06 ± 0.042^{B}	EJ 7.0 ± 6.0 (2) GR 16.6 ± 3.2^{P} (10)	0.065 ± 0.045^{A}	0.160 ± 0.05^{B}	0.22 ± 0.0^{B}	14.4 ± 3.2^{B}
Non–TX-BC	63	0.216 ± 0.008^{C}	1.8 ± 0.06^{B}	0.17 ± 0.06^{B}	NA	0.08 ± 0.04^{A}	0.43 ± 0.070^{B}	0.36 ± 0.07^{B}	29.4 ± 3.3^{B}

*t test and **Fisher's exact test: Column values (mean ± SE) with different superscript letters (A to D; except GR sperm, which is N and P) are significantly different ($P < 0.05$). §From (*7*).

spite of improvements, ongoing density-dependent factors (related to limited and decreasing habitat availability) and stochastic events will continue to regulate population growth, requiring continued commitments to identify and maintain additional quality habitat to preserve Florida panther evolutionary potential for the long term.

References and Notes

1. M. J. Currier, *Mamm. Species* **200**, 1 (1983).
2. R. T. McBride, R. T. McBride, R. M. McBride, C. E. McBride, *Southeast. Nat.* **7**, 381 (2008).
3. S. J. O'Brien *et al.*, *Natl. Geogr. Res.* **6**, 485 (1990).
4. M. E. Roelke, J. S. Martenson, S. J. O'Brien, *Curr. Biol.* **3**, 340 (1993).
5. M. Culver, W. E. Johnson, J. Pecon-Slattery, S. J. O'Brien, *J. Hered.* **91**, 186 (2000).
6. P. W. Hedrick, R. Fredrickson, *Conserv. Genet.* **11**, 615 (2010).
7. M. A. Barone *et al.*, *J. Mammal.* **75**, 150 (1994).
8. M. W. Cunningham *et al.*, *J. Wildl. Dis.* **35**, 519 (1999).
9. M. E. Roelke *et al.*, *J. Wildl. Dis.* **29**, 36 (1993).
10. M. W. Cunningham *et al.*, *J. Wildl. Dis.* **44**, 537 (2009).
11. U. S. Seal, R. C. Lacy, Eds., *A Plan for Genetic Restoration and Management of the Florida Panther* (*Felis concolor coryi*) (Report to the Florida Game and Fresh Water Fish Commission, Conservation Breeding Specialist Group, Apple Valley, MN, 1994).
12. S. J. O'Brien, *Tears of the Cheetah and Other Tales from the Genetic Frontier* (St. Martin's Press, New York, 2003).
13. Materials, methods, and additional figures and tables are available as supporting material on *Science* Online.
14. M. E. Roelke *et al.*, *J. Wildl. Dis.* **42**, 234 (2006).
15. R. C. Lacy, *J. Mammal.* **78**, 320 (1997).
16. P. W. Hedrick, S. T. Kalinowski, *Annu. Rev. Ecol. Syst.* **31**, 139 (2000).
17. R. Frankham, K. Ralls, *Nature* **392**, 441 (1998).

18. R. Lande, *Science* **241**, 1455 (1988).
19. M. Culver, P. W. Hedrick, K. Murphy, S. O'Brien, M. G. Hornocker, *Anim. Conserv.* **11**, 104 (2008).
20. S. J. O'Brien, E. Mayr, *Science* **251**, 1187 (1991).
21. M. W. Janis, J. D. Clark, *J. Wildl. Manage.* **66**, 839 (2002).
22. M. L. Foster, S. R. Humphrey, *Wildl. Soc. Bull.* **23**, 95 (1995).
23. R. Kautz *et al.*, *Biol. Conserv.* **130**, 118 (2006).
24. We dedicate this study to the memory of Ulysses Seal and Ernst Mayr, important heroes in the conservation struggle of the Florida panther. Funded by the Florida Fish and Wildlife Conservation Commission (FWC) via purchases of Florida panther license plates. Other major funding for the field work was provided by Everglades National Park (EVER), the BCNP, and federal funds from the U.S. Fish and Wildlife Service (especially in the early years) as well as from the National Cancer Institute, National Institutes of Health (NIH), under contract number N01-CO-12400. This research was supported in part by the Intramural Research Program of NIH, National Cancer Institute, Center for Cancer Research, and the Florida Panther Research and Management Trust Fund. All panther captures, sampling, and radio collaring were authorized by U.S. Fish and Wildlife Service Endangered Species Permits TE01553-3 (FWC) and TE146761-1 (BCNP). We thank many individuals for their help in this project, who are named in SOM reference S25.

Supporting Online Material

www.sciencemag.org/cgi/content/full/329/5999/1641/DC1
Materials and Methods
Figs. S1 to S5
Tables S1 to S6
References

27 May 2010; accepted 11 August 2010
10.1126/science.1192891

Parasympathetic Innervation Maintains Epithelial Progenitor Cells During Salivary Organogenesis

S. M. Knox,[1] I. M. A. Lombaert,[1] X. Reed,[1] L. Vitale-Cross,[2] J. S. Gutkind,[2] M. P. Hoffman[1]*

The maintenance of a progenitor cell population as a reservoir of undifferentiated cells is required for organ development and regeneration. However, the mechanisms by which epithelial progenitor cells are maintained during organogenesis are poorly understood. We report that removal of the parasympathetic ganglion in mouse explant organ culture decreased the number and morphogenesis of keratin 5–positive epithelial progenitor cells. These effects were rescued with an acetylcholine analog. We demonstrate that acetylcholine signaling, via the muscarinic M1 receptor and epidermal growth factor receptor, increased epithelial morphogenesis and proliferation of the keratin 5–positive progenitor cells. Parasympathetic innervation maintained the epithelial progenitor cell population in an undifferentiated state, which was required for organogenesis. This mechanism for epithelial progenitor cell maintenance may be targeted for organ repair or regeneration.

Organogenesis involves the coordinated growth of epithelium, mesenchyme, nerves, and blood vessels, which use common sets of genes, guidance cues, and growth factor–signaling pathways (*1*–*5*). Research on epithelial organogenesis has focused on epithelial-mesenchymal and endothelial-epithelial cell interactions. However, the function of the peripheral nervous system during epithelial organogenesis is less clear.

Pavlov's seminal experiments on dogs demonstrated that neuronal input controls salivary gland function (*6*), and more recent work showed that parasympathetic innervation of salivary glands is essential for regeneration after injury (*7*). Because parasympathetic innervation occurs in parallel with salivary gland development (*8*), we hypothesized that parasympathetic innervation is required for epithelial progenitor cell function during organogenesis.

To test this hypothesis, we used mouse embryonic submandibular gland (SMG) explant culture and mechanically removed the parasympathetic submandibular ganglion (PSG) before the gland developed (*9*). SMG development begins at embryonic day 11 (E11), when the oral epithelium invaginates into neural crest–derived mesenchyme (*10*). The neuronal bodies of the PSG condense around the epithelium at E12 (fig. S1A) and could be separated from epithelium and mesenchyme in explant culture. When the separated tissues were recombined in culture, the growth of the SMG epithelium was reduced, with a significant decrease in the number of end buds in the absence of the PSG (Fig. 1, A and B, and fig. S2A). The PSG axons have abundant varicosities (fig. S2B, box) that contain the neurotransmitter acetylcholine (ACh) (*8*), and express the ACh synthetic enzyme (*Chat*) (fig. S1, B and C). ACh activates epithelial muscarinic (M) receptors, and M1 (*Chrm1*) is the major muscarinic receptor in the embryonic SMG epithelium (fig. S1, B and C), whereas M1 and M3 (*Chrm3*) stimulate saliva secretion in the adult (*7*). Alternatively, we perturbed ACh/M1 signaling using the chemical inhibitors, 4-DAMP (DAMP; *N*-2-chloroethyl-4-piperidinyl diphenylacetate), an irreversible M1/M3 inhibitor (Fig. 1C); atropine, a competitive muscarinic antagonist (fig. S2D); beta-bungarotoxin (Btx), which depletes neuronal ACh stores (fig. S2E); and small interfering RNA (siRNA) to M1 (*Chrm1*) (fig. S2, H to I). All treatments reduced the number of end buds (fig. S2, C to I). In contrast, inhibition of α_2-adrenergic receptors with idazoxan had no effect (fig. S2F). These experiments demonstrate that epithelial morphogenesis requires PSG, ACh, and M1 activity.

Epithelial morphogenesis may also depend on the size of the epithelial progenitor pool and growth factor–mediated proliferation (*11*). To distinguish between these two possibilities, we mea-

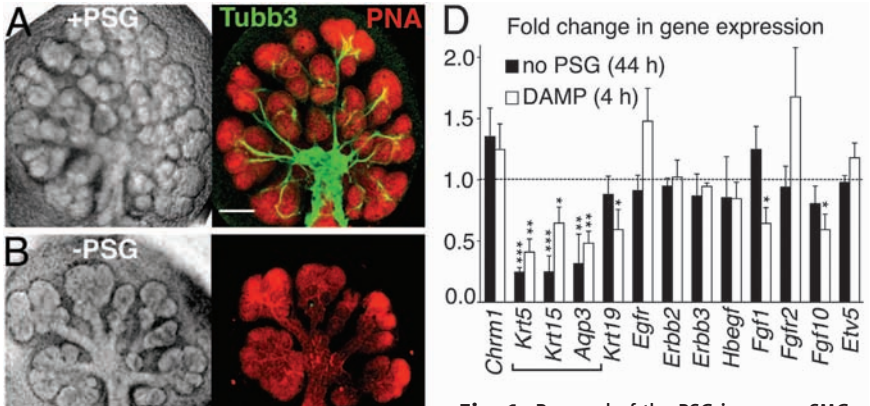

Fig. 1. Removal of the PSG in mouse SMG explant culture decreases branching morphogenesis and expression of basal progenitor cell markers. SMGs were cultured for 44 hours, (**A**) with or (**B**) without the PSG or (**C**) treated with a muscarinic inhibitor (DAMP). Whole-mount images of the nerves (β3-tubulin, Tubb3) and the epithelium (peanut agglutinin, PNA) are shown. Scale bar, 200 μm. (**D**) Quantitative polymerase chain reaction (QPCR) analysis of gene expression. Means ± SEM of three experiments. Student's *t* test; $*P < 0.05$, $**P < 0.01$, $***P < 0.001$.

[1]Matrix and Morphogenesis Unit, Laboratory of Cell and Developmental Biology, National Institute of Dental and Craniofacial Research, NIH, 30 Convent Drive, Bethesda, MD 20892, USA. [2]Oral and Pharyngeal Cancer Branch, National Institute of Dental and Craniofacial Research, NIH, 30 Convent Drive, Bethesda, MD 20892, USA.

*To whom correspondence should be addressed. E-mail: mhoffman@mail.nih.gov